

Maternal–fetal transfer rates of PCBs, OCPs, PBDEs, and dioxin-like compounds predicted through quantitative structure–activity relationship modeling

Akifumi Eguchi¹ · Masamichi Hanazato² · Norimichi Suzuki² · Yoshiharu Matsuno² · Emiko Todaka² · Chisato Mori^{2,3}

Received: 1 February 2015 / Accepted: 15 September 2015 / Published online: 23 September 2015
© Springer-Verlag Berlin Heidelberg 2015

Abstract The present study aims to predict the maternal–fetal transfer rates of the polychlorinated biphenyls (PCBs), organochlorine pesticides (OCPs), and polybrominated diphenyl ethers (PBDEs), and dioxin-like compounds using a quantitative structure–activity relationship model. The relation between the maternal–fetal transfer rate and the contaminants' physicochemical properties was investigated by multiple linear regression (MLR), partial least square regression (PLS), and random forest regression (RF). The 10-fold cross-validation technique estimated low predictive performances for both MLR and PLS models ($R^2_{CV}=0.425\pm 0.0964$ for MLR and $R^2_{CV}=0.492\pm 0.115$ for PLS) and is in agreement with an external test ($R^2_{pred}=0.129$ for MLR and $R^2_{pred}=0.123$ for PLS). In contrast, the RF model exhibits good predictive performance, estimated through 10-fold cross-validation ($R^2_{CV}=0.566\pm 0.0885$) and an external test set ($R^2_{pred}=0.519$). Molecular weight and polarity were selected in all models as important parameters that may predict the ability of a molecule to cross the placenta to the fetus.

Keywords POPs · Dioxins · Maternal transfer rate · QSAR

Introduction

In Japan, polychlorinated biphenyls (PCBs), organochlorine pesticides (OCPs), and polybrominated diphenyl ethers (PBDEs) have been detected in human fetuses and human serum, despite the ban or restriction of their use (Fukata et al. 2005; Kawashiro et al. 2008; Mori et al. 2014). Highly lipophilic and stable, these compounds have a long residence time in human tissues; they have been detected in cord blood (Aylward et al. 2014), indicating that fetuses were exposed to them through the blood stream. Congeners of dioxin include polychlorinated dibenzo-p-dioxins (PCDDs), polychlorinated dibenzofurans (PCDFs), and dioxin-like polychlorinated biphenyls (DL-PCBs); they affect human reproduction and development because of their endocrine-disrupting effects (Ankley et al. 2010; Brouwer et al. 1995; Mably et al. 1992). Experimental epidemiological studies also suggest that PCBs, OCPs, and PBDEs have developmental neurotoxicity (Grandjean and Landrigan 2006, 2014). Thus, it is important to determine the mechanisms by which these compounds are transported from the mother to the fetus.

In the present study, the maternal–fetal transfer rate of PCBs, OCPs, PBDEs, and dioxin-like compounds is predicted using multivariate analysis to detect relations between the compounds' physicochemical properties and their concentrations in maternal blood (MB) and umbilical cord blood (CB) (Jotaki et al. 2011; Kawashiro et al. 2008; Mori et al. 2014; Sakurai et al. 2004). Previous studies have reported ratios of cord/maternal blood concentrations of PCBs, OCPs, PBDEs, and dioxin-like compounds between 0.1 and 1 (Aylward et al. 2014). In cases of fetal exposure to higher chlorinated congeners of PCBs or dioxins with larger molecular weights, the

Responsible editor: Roland Kallenborn

Electronic supplementary material The online version of this article (doi:10.1007/s11356-015-5436-0) contains supplementary material, which is available to authorized users.

✉ Akifumi Eguchi
a_eguchi@chiba-u.jp

¹ Clinical Cell Biology and Medicine, Graduate School of Medicine, Chiba University, Chuo-ku Inohana 1-8-1, Chiba City, Japan

² Center for Preventive Medical Sciences, Chiba University, Inage-ku Yayoi-cho 1-33, Chiba City, Japan

³ Department of Bioenvironmental Medicine, Graduate School of Medicine, Chiba University, Chuo-ku Inohana 1-8-1, Chiba City, Japan

transfer rate would be lower (Mori et al. 2014; Needham et al. 2011). However, correlations between the maternal–fetal transfer rate and the compounds' physicochemical properties are still not well understood. The quantitative structure–activity relationship (QSAR) method enables to predict the physicochemical properties or the theoretical molecular descriptors of chemicals, from their molecular structure. The QSAR method has been applied before to investigate the placental barrier for some organic compounds (Hewitt et al. 2007). However, transfer rates of organohalogen compounds, including dioxin-like compounds, could not be estimated.

Materials and methods

Sample acquisition, processing, and analysis

The MB and CB sample sets ($n=79$) were collected from the Chiba University Hospital's Delivery Unit and various other obstetric units in Japan, after the approval of this study by the Congress of Medical Bioethics of Chiba University and with the written and informed consent of the patients. The samples were stored at $-20\text{ }^{\circ}\text{C}$. The concentrations of PCBs (TriCB, TetraCB, PentaCB, HexaCB, HeptaCB, OctaCB, NonaCB, and DecaCB) and OCPs (trans-nonachlor, hexachlorocyclohexane, hexachlorobenzene, and heptachlor epoxide) were analyzed in 29 sample sets using an Agilent 6890 Plus gas chromatography (Agilent Technologies) and an AutoSpec Ultima NT mass spectrometer (Micromass Ltd., Manchester, UK) equipped with a programmed temperature vaporization (PTV) injection system (Agilent Technologies, Palo Alto, CA, USA) (Jotaki et al. 2011). The analytical method of Sakurai et al. (2004) was employed in 41 sample sets for dioxin-like compounds (polychlorinated dibenzo-*p*-dioxins (PCDDs), polychlorinated dibenzofuran (PCDFs), and dioxin-like polychlorinated biphenyl (DL-PCBs). These compounds were analyzed by high-resolution gas chromatography/high-resolution mass spectrometry (HRGC-HRMS). PBDEs' (BDE47, 100, 153) analysis in nine samples was also conducted using HRGC-HRMS (Kawashiro et al. 2008).

Statistical analysis and modeling

A possible association of the maternal transfer rate with the contaminants' physicochemical properties was investigated by multiple linear regression (MLR), partial least square (PLS) regression, and random forest (RF) regression.

Maternal–fetal transfer rates were assigned by dividing the concentration of organohalogen compounds in maternal blood and cord serum (Table 1). In addition, Table 1 presents other related physicochemical properties: biodegradation half-life, logarithm bioaccumulation factor (logBAF), logarithm bioconcentration factor (logBCF), logarithm octanol/water

partition coefficient (logKow), logarithm octanol/air partition coefficient (logKoA), and water solubility. The following quantum-chemical descriptors were acquired for the QSAR model: molecular weight, final formation heat, energy of the highest occupied molecular orbital (E_{HOMO}), energy of the lowest unoccupied molecular orbital (E_{LUMO}), HOMO–LUMO gap, greatest negative partial atomic charge (q^-), greatest positive partial atomic charge (q^+), total dipole, total energy, electronic energy, and core–core repulsion (Table 1). These quantum-chemical descriptors were obtained by the PM6 semiempirical method contained in MOPAC 2009 (Ver 9.03CS) (Stewart 2007, 2009), which was implemented in ChemBioOffice 2013 (Cambridge Soft Corporation, USA). The biodegradation half-life, logBAF, logBCF, logKow, and water solubility were drawn from the Estimation Program Interface (EPI) Suite (United States Environmental Protection Agency, Washington, DC, USA) (EPA 2012). The quantum-chemical descriptors and physicochemical properties of the TetraCB, PentaCB, HexaCB, HeptaCB, and OctaCB isomers were used as CB74, CB118, CB153, CB180, and CB194, respectively. Furthermore, the toxic equivalency factor (TEF) was used as a descriptor for the present analysis (Van den Berg et al. 2006).

Statistical analysis was performed using R Ver. 3.1.1 (The R Foundation for Statistical Computing), and SIMCA 13 (Umetrics, Umeå, Sweden). Before statistical analysis, all values were standardized using the equation:

$$z = (x - \mu) / \sigma$$

where μ is the mean and σ is the standard deviation of the variables.

Principal component analysis (PCA) was employed to order the physicochemical and structure properties and the maternal–fetal transfer rates (Fig. 1). Spearman's rank correlation was performed to identify collinear variables in physicochemical and structural properties (Table 2); one variable was exempt from the analysis for every given pair of descriptors exhibiting a correlation coefficient value greater than 0.7.

A dataset of individual maternal–fetal transfer rates, containing 29 pairs of each isomer of PCBs and OCPs, 41 pairs of each congener of dioxin-like compounds, and 8 pairs of each congener of PBDEs, was used for developing the prediction models (Tables S1 and S2). Individual maternal–fetal transfer rates were calculated by dividing the concentration of each chemical in CB by its concentration in MB for each pairs of CB and MB. MLR, PLS regression, and RF regression were applied. The multicollinearity of the independent variables was assessed by calculating the variance inflation factor (VIF) for MLR; the explanatory variables' VIF values were <5 , indicating a rejection of multicollinearity. The parameters optimizing likelihood were identified after variable selection by Spearman's rank correlation and VIF calculation. The

Table 1 Summary of maternal–fetal transfer rates and physicochemical properties of organohalogen compounds

Compound	Smiles	Type	Transfer rate	Molecular weight	TEF	LogKow	LogKoA	Water solubility	LogBCF	LogBAF	Half-life
HCB	Clc1=cc(Cl)c(Cl)c(Cl)c(Cl)c1	Training	0.27	284.78	0	5.86	6.888	0.192	4.201	5.898	21.53
HCH	Cl(C(C(C(C1)C1)C1)C1)C1	Training	0.2	290.83	0	4.26	7.817	4.04	3.121	3.287	8.84
Trans-nonachlor	Cl2C(C(C1)C1)C1C3(C(C(C2)C3(C1)C1)C1)C1C1C1	Test	0.217	444.22	0	6.44	9.344	0.00612	4.182	6.443	217.6
Heptachlor epoxide	Cl2C(C(C3)O3)C1C4(C(C(C2)C4(C1)C1)C1)C1C1	Training	0.187	389.32	0	4.56	8.046	0.199	3.835	4.747	33.71
1.2.3.7.8.PeCDD	Cl=C2C(C(C1)C1)OC3=C(C(C(C3O2)C1)C1)C1	Training	0.231	356.42	1	7.56	10.57	0.000939	3.736	5.713	9.629
1.2.3.6.7.8.HxCDD	Cl=C2C(C(C1)C1)OC3=CC(C(C3O2)C1)C1C1	Training	0.218	390.86	0.1	8.21	12.31	2.65E-05	2.26	4.68	30.82
1.2.3.4.6.7.8.HpCDD	Cl=C2C(C(C1)C1)OC3=C(O2)C(C(C3)C1)C1C1	Training	0.186	425.31	0.01	8.85	10.15	2.44E-05	2.455	4.825	28.04
OCDD	Cl2=C(C(C(C1)C1)C1)OC3=C(C(C(C3)C1)C1)C1	Training	0.109	495.75	0.0003	9.5	11.76	9.97E-06	2.222	4.565	34.08
2.3.4.7.8.PeCDF	Cl=C2C3=CC(C(C1)C1)OC2=CC(C1)C1C1C1C1	Training	0.216	340.42	0.3	7.27	10.7	0.000339	2.827	4.41	8.533
1.2.3.6.7.8.HxCDF	Cl=C2C3=C(C(C=C3OC2=C(C(C1)C1)C1)C1)C1	Test	0.302	374.87	0.1	7.92	11.48	0.000349	2.337	4.353	14.2
1.2.3.4.7.8.HxCDF	Cl=C2C(C(C1)C1)OC3=C2C(C(C=C3)C1)C1C1	Test	0.251	374.87	0.1	7.92	11.48	0.000349	2.477	4.734	14.2
1.2.3.4.6.7.8.HpCDF	Cl=C2C3=C(C(C(C3)C1)C1)OC2=C(C(C=C1)C1)C1	Training	0.326	409.31	0.01	8.56	12.25	1.02E-05	2.076	4.775	23.63
CB77	Cl=CC(C(C=C1)C2=CC(C(C=C2)C1)C1)C1	Training	0.328	291.99	0.0001	6.34	10.05	0.0298	3.59	5.301	213.6
CB126	Cl=CC(C(C=C1)C2=CC(C(C=C2)C1)C1)C1	Training	0.184	326.44	0.1	6.98	9.403	0.00939	3.957	6.798	288.5
CB169	Cl=C(C(C(C1)C1)C1)C2=CC(C(C=C2)C1)C1C1	Training	0.146	360.88	0.03	7.62	9.963	0.0025	3.755	6.959	412.6
CB105	Cl=CC(C(C=C1)C2=C(C(C=C2)C1)C1)C1	Test	0.196	326.44	0.00003	6.98	9.234	0.0134	4.06	6.768	254.1
CB114	Cl=CC(C(C=C1)C2=CC(C(C=C2)C1)C1)C1	Training	0.195	326.44	0.00003	6.98	9.403	0.00939	3.947	6.776	288.5
CB118	Cl=CC(C(C=C1)C2=CC(C(C=C2)C1)C1)C1	Training	0.198	326.44	0.00003	6.98	9.049	0.00713	3.811	6.678	318.6
CB123	Cl=CC(C(C=C1)C1)C2=CC(C(C=C2)C1)C1C1	Training	0.217	326.44	0.00003	6.98	9.049	0.00713	3.811	6.678	318.6
CB156	Cl=CC(C(C=C1)C2=CC(C(C=C2)C1)C1)C1	Training	0.158	360.88	0.00003	7.6	9.833	0.00533	3.663	6.993	472
CB157	Cl=CC(C(C=C1)C2=CC(C(C=C2)C1)C1)C1	Training	0.18	360.88	0.00003	7.6	10.15	0.00172	3.651	6.972	472
CB167	Cl=C(C(C(C1)C1)C1)C2=CC(C(C=C2)C1)C1	Training	0.175	360.88	0.00003	7.5	10.05	0.00223	3.653	6.864	439.8
CB189	Cl=C(C(C=C1)C1)C2=CC(C(C=C2)C1)C1C1	Test	0.131	395.33	0.00003	8.27	10.95	0.000753	3.063	6.506	799
TetraCB	Cl=CC(C(C=C1)C2=CC(C(C=C2)C1)C1)C1	Training	0.235	291.99	0	6.34	9.058	0.0275	4.133	6.752	219.7
PentaCB	Cl=CC(C(C=C1)C2=CC(C(C=C2)C1)C1)C1	Training	0.197	326.44	0	6.98	9.049	0.00713	3.811	6.678	318.6
HexaCB	Cl=C(C(C=C1)C1)C2=CC(C(C=C2)C1)C1	Training	0.186	360.88	0	7.62	10.78	0.00128	3.525	6.888	524.9
HeptaCB	Cl=C(C(C=C1)C1)C2=CC(C(C=C2)C1)C1C1	Test	0.157	395.33	0	8.27	11.66	0.000284	3.277	6.848	799
OctaCB	Cl=C(C(C=C1)C1)C1)C2=CC(C(C=C2)C1)C1C1	Training	0.124	429.77	0	8.91	12.07	7.72E-05	2.994	6.624	1128
BDE47	Cl=CC(C(C=C1)Br)OC2=C(C(C=C2)Br)Br	Training	0.359	485.71	0	6.77	10.69	0.00146	3.699	5.829	36.03
BDE100	Cl=CC(C(C=C1)Br)OC2=C(C(C=C2)Br)Br	Test	0.139	563.62	0	7.66	11.98	7.86E-05	3.2	6.107	57.26
BDE153	Cl=C(C(C=C1)Br)OC2=CC(C(C=C2)Br)Br	Training	0.136	643.53	0	8.55	13.27	4.15E-06	2.624	5.951	91

Compound	Final heat of formation	Total energy	Electronic energy	Core–core repulsion	E_{HOMO}	E_{LUMO}	q^-	q^+	$E_{\text{HOMO}}-E_{\text{LUMO}}$	Total dipole
HCB	-10.02	-2261.11	-10,722.06	8460.95	-9.829	-1.427	-0.014822	0.014803	-8.402	0
HCH	-67.25	-2344.63	-12,521.6	10,176.97	-11.191	-0.484	-0.107879	0.190558	-10.707	0.003
Trans-nonachlor	-46.23	-3583.16	-25,246.26	21,663.1	-10.166	-1.068	-0.153951	0.198841	-9.098	0.255
Heptachlor epoxide	-26.01	-3363.66	-22,617.76	19,254.11	-10.21	-1.061	-0.372118	0.192382	-9.149	2.131
1.2.3.7.8.PeCDD	-41.1	-3363.9	-20,171.04	16,807.15	-9.018	-1.399	-0.283815	0.205684	-7.619	0.784
1.2.3.6.7.8.HxCDD	-44.17	-3604.69	22,182.22	18,577.53	-9.099	-1.503	-0.262225	0.20768	-7.596	0
1.2.3.4.6.7.8.HpCDD	-46.82	-3845.47	-24,313.78	20,468.31	-9.164	-1.605	-0.261116	0.20757	-7.559	0.702

Table 1 (continued)

Compound	Final heat of formation	Total energy	Electronic energy	Core-core repulsion	E_{HOMO}	E_{LUMO}	q^-	q^+	$E_{\text{HOMO}}-E_{\text{LUMO}}$	Total dipole
OCDD	-49.46	-4086.24	-26,509.76	22,423.52	-9.235	-1.696	-0.240525	0.128799	-7.539	0
2.3.4.7.8.PeCDF	-10.13	-3072.85	-18,074.85	15,002.01	-9.451	-1.647	-0.253212	0.204659	-7.804	0.828
1.2.3.6.7.8.HxCDF	-14.97	-3313.72	-20,059.63	16,745.91	-9.539	-1.76	-0.278261	0.265523	-7.779	0.549
1.2.3.4.7.8.HxCDF	-14.69	-3313.7	-20,071.41	16,757.7	-9.428	-1.776	-0.248272	0.223125	-7.652	0.079
1.2.3.4.6.7.8.HpCDF	-17.23	-3554.47	-22,048.33	18,493.86	-9.495	-1.89	-0.211466	0.215083	-7.605	0.779
CB77	14.9	-2568.4	-14,630.06	12,061.66	-9.487	-1.016	-0.176338	0.180532	-8.471	1.156
CB126	9.429	-2809.3	-16,307.26	13,497.96	-9.596	-1.197	-0.204368	0.186775	-8.399	1.295
CB169	4.069	-3050.19	-18,041.51	14,991.32	-9.7	-1.354	-0.197114	0.186672	-8.346	0.004
CB105	10.17	-2809.27	-16,549.59	13,740.33	-9.536	-1.142	-0.171757	0.179729	-8.394	1.889
CB114	10.7	-2809.24	-16,586.67	13,777.42	-9.537	-1.208	-0.18435	0.188443	-8.329	0.943
CB118	7.148	-2809.4	-16,487.12	13,677.72	-9.516	-1.195	-0.181814	0.193855	-8.321	1.397
CB123	6.866	-2809.41	-16,531.61	13,722.19	-9.584	-1.159	-0.221646	0.194447	-8.425	2.199
CB156	5.166	-3050.15	-18,326.41	15,276.27	-9.607	-1.339	-0.173688	0.188164	-8.268	1.65
CB157	4.784	-3050.16	-18,323.55	15,273.38	-9.654	-1.294	-0.200036	0.189813	-8.36	2.272
CB167	1.771	-3050.29	-18,254.88	15,204.59	-9.624	-1.339	-0.185954	0.194953	-8.285	1.242
CB189	-0.178	-3291.04	-20,139.83	16,848.8	-9.704	-1.473	-0.193045	0.189624	-8.231	1.03
TetraCB	12.84	-2568.49	-14,823.81	12,255.32	-9.444	-1.05	-0.182573	0.192774	-8.394	0.104
PentaCB	7.148	-2809.4	-16,487.12	13,677.72	-9.516	-1.195	-0.181814	0.193855	-8.321	1.397
HexaCB	-0.638	-3050.4	-18,472.46	15,422.06	-9.564	-1.314	-0.186678	0.194539	-8.25	0.161
HeptaCB	-2.617	-3291.14	-20,378.12	17,086.98	-9.645	-1.441	-0.188667	0.19527	-8.204	0.992
OctaCB	-4.534	-3531.89	-22,341.39	18,809.5	-9.728	-1.556	-0.149975	0.191711	-8.172	0.894
BDE47	28.69	-2753.33	-16,575.57	13,822.24	-9.378	-0.918	-0.356675	0.298169	-8.46	0.845
BDE100	34.36	-2967.7	-18,335.42	15,367.72	-9.453	-1.109	-0.336447	0.301132	-8.344	0.663
BDE153	39.54	-3182.09	-19,788.16	16,606.08	-9.616	-1.281	-0.345929	0.304055	-8.335	0.445

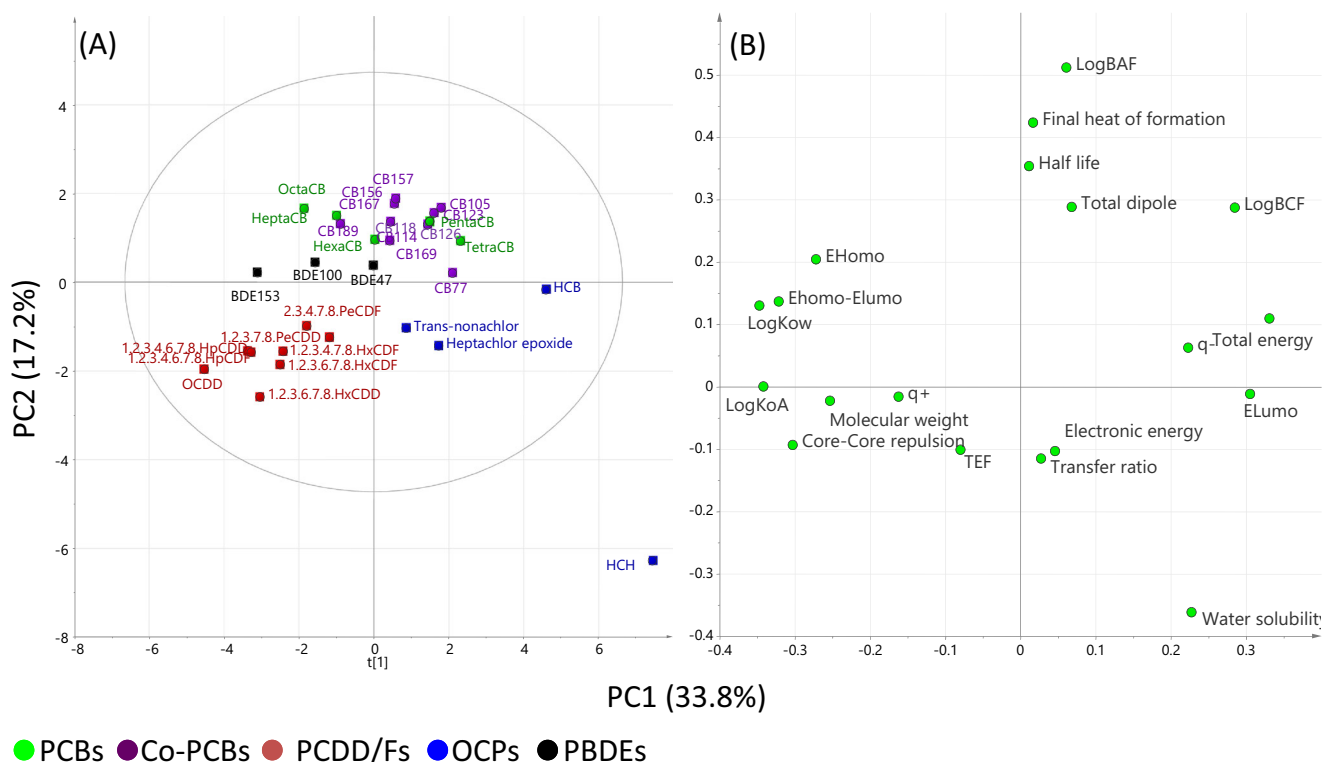


Fig. 1 The physicochemical properties of PCBs, OCPs, PBDEs, and dioxin-like compounds. **a** PCA loading plot and **b** score plot

optimized likelihoods from different models were then compared using the Akaike information criterion (AIC) (Akaike 1998):

$$\text{AIC} = 2k - 2\ln L$$

where k represents the number of parameters and L represents maximized likelihood. The model with the lowest AIC was selected to achieve a trade-off between model complexity (preferring models with fewer parameters) and maximized likelihood.

PLS regression is widely used in chemometrics for model development because PLS can analyze data with strong collinear and multiple predictor variables (Wold et al. 2001). RF is a generalized regression method, which is effective in various QSAR tasks; every forest represents a consensus, nonlinear model derived from a large number of single models (Breiman 2001).

PLS and RF were obtained using the R package. Hyperparameters, $mtry$ for RF (number of variables randomly sampled as candidates in each split) and the number of components for PLS, were optimized by the R package caret (Kuhn 2008). The R package caret was also used to calculate the variable importance for each model. In all cases, the training set contained 80 % of compounds (24 compounds [HCB, HCH, heptachlor epoxide, 1,2,3,7,8-PeCDD, 1,2,3,6,7,8-HxCDD, 1,2,3,4,6,7,8-HpCDD, OCDD, 2,3,4,7,8-PeCDF, 1,2,3,4,6,7,8-HpCDF, CB77, CB126, CB169, CB114, CB118, CB123, CB156, CB157, CB167, TetraCB, PentaCB, HexaCB,

OctaCB, BDE47, and BDE153]), and the external test sets comprised 20 % of compounds (7 compounds [trans-nonachlor, 1,2,3,4,7,8-HxCDF, 1,2,3,6,7,8-HxCDF, CB105, CB189, HeptaCB, and BDE100]) (Tables S1 and S2). The external validation test set was randomly selected from each type of organohalogen compound (PCDD/Fs, coplanar PCBs, PCBs, organohalogen pesticide, and PBDEs). Models were optimized by 10-fold cross-validation using a training set for internal validation. Optimized $mtry=1$ and the number of components=9, for RF and PLS, respectively. Optimized models were validated by external test sets. The root mean square error (RMSE), the correlation coefficient (R^2), and the correlation coefficient's standard deviation (SD) were reported for cross-validation testing set ($RMSE_{CV}$, R^2_{CV} , and SD_{CV}) and between predicted and actual values of the response variable of the test data ($RMSE_{pred}$ and R^2_{pred}). Tropsha's validation factor " R^2_{ext} ," " k ," and " $(R^2_{ext} - R^2_0)/R^2_{ext}$ " were also calculated, and the applicability domain and y -randomization were entered for the RF model (Tropsha 2010). The RMSE, k , and R^2_0 were calculated by the following equations:

$$\text{RMSE} = \sqrt{\frac{1}{N} \sum_{i=1}^N (y_{exp} - y_{pred})^2}$$

$$R^2_{EXT} = 1 - \frac{\sum_{I=1}^N (y_{pred} - y_{exp})^2}{\sum_{I=1}^N (y_{pred} - \bar{y}_{cv})^2}$$

Table 2 Intercorrelation matrix of the physicochemical properties of organohalogen compounds

	Molecular weight	TEF	LogKow	LogKoa	Water solubility	LogBCF	LogBAF	Half-life	Final heat of formation	Total energy	Electronic energy	Core-core repulsion	E_{HOMO}	E_{LUMO}	q^-	q^+	E_{HOMO}	E_{LUMO}	Total dipole	
Molecular weight	1.00																			
TEF	-0.08	1.00																		
LogKow	0.68	0.31	1.00																	
LogKoa	0.74	0.25	0.84	1.00																
Water solubility	- 0.79	-0.27	- 0.92	- 0.91	1.00															
LogBCF	-0.55	-0.35	- 0.77	- 0.80	0.81	1.00														
LogBAF	-0.19	-0.26	-0.05	-0.02	0.24	0.52	1.00													
Half-life	0.03	-0.36	0.15	-0.02	0.07	0.26	0.85	1.00												
Final heat of formation	-0.17	-0.28	-0.23	-0.09	0.23	0.39	0.53	0.43	1.00											
Total energy	- 0.71	-0.33	- 0.71	-0.61	0.74	0.59	0.32	0.12	0.65	1.00										
Electronic energy	- 0.74	-0.03	-0.59	-0.47	0.58	0.39	0.13	-0.03	0.43	0.79	1.00									
Core-core repulsion	0.82	0.14	0.68	0.62	-0.71	-0.54	-0.26	-0.03	-0.57	- 0.95	- 0.87	1.00								
E_{HOMO}	0.09	0.49	0.24	0.34	-0.38	-0.32	-0.32	-0.41	0.05	-0.16	0.05	0.08	1.00							
E_{LUMO}	-0.33	-0.56	- 0.77	-0.6	0.70	0.64	0.23	0.14	0.50	0.66	0.45	-0.54	-0.21	1.00						
q^-	-0.53	-0.34	-0.34	-0.49	0.52	0.42	0.38	0.39	0.04	-0.43	0.32	-0.42	-0.45	0.21	1.00					
q^+	0.54	-0.04	0.32	0.53	0.58	-0.45	-0.35	-0.34	-0.06	-0.4	-0.29	0.38	0.37	-0.17	-0.63	1.00				
E_{HOMO}	0.39	0.53	0.83	0.67	- 0.79	- 0.7	-0.21	-0.10	-0.41	-0.69	-0.45	0.58	0.52	- 0.87	-0.30	0.32	1.00			
E_{LUMO}																				
Total dipole	-0.20	-0.05	-0.21	-0.30	0.31	0.34	0.46	0.48	0.41	0.22	0.03	-0.18	-0.19	0.30	0.06	-0.20	-0.25	1.00		

Factors having high intercorrelation greater than 0.7 (shown as bold) were subjected to removal

where

$$\overline{y_{cv}}$$

is the mean overall predictive values by R^2_{cv}

$$k = \frac{\sum_{i=1}^N y_{exp}^* y_{pred}}{\sum_{i=1}^N y_{pred}^2}$$

$$R^2_0 = 1 - \frac{\sum_{I=1}^N (y_{pred} - K^* y_{exp})^2}{\sum_{I=1}^N (y_{pred} - \overline{y_{exp}})^2}$$

, where

$$\overline{y_{exp}}$$

is the mean overall predictive values by R^2_{pred} Tropsha considered a QSAR model predictive if the following conditions are satisfied (Tropsha 2010):

$$R^2_{pred} > 0.6$$

$$R^2_{EXT} > 0.5$$

$$(R^2_{ext} - R^2_0) / R^2_{ext} < 0.1$$

$$0.85 \leq k \leq 1.15$$

The averaged y -randomized R^2 (R^2_{random}) was calculated after 100 randomized iterations to check the reliability of the proposed model (Rucker et al. 2007). The dependent variable vector is randomly shuffled, and a new QSAR model is developed using the original independent variable matrix. If the new QSAR models are expected to have lower R^2 values than the proposed mode, the proposed model might be acceptable (Rucker et al. 2007; Tropsha 2010).

Finally, the distance of a test set was calculated to its nearest neighbor in the training set and compared to the APD threshold, calculated as follows:

$$APD = \langle d \rangle + Z\sigma \quad [Z: \text{empirical cutoff value } 0.5 \text{ (Zhang et al. 2006)}]$$

The prediction was considered unreliable when the distance was higher than the APD. Calculation of $\langle d \rangle$ and σ was performed as follows: First, the average of the Euclidean distances between all pairs of the training set was calculated. Next, the set of distances that were lower than the average was formulated. $\langle d \rangle$ and σ were finally calculated as the average and standard deviation of all the distances included in this set (Zhang et al. 2006).

This analysis included only the contaminants that were detected in at least 80 % of the samples. All values were standardized and scaled to zero mean and unit variance before all statistical analysis. Results below limit of quantification (LOQ) were assigned a value of 0.5 LOQ.

Results

Ordination of the compounds' physicochemical properties

PCA was applied to summarize profiles of physicochemical properties of PCBs, OCPs, PBDEs, and dioxin-like compounds as well as to examine the relation with transfer rate; the results are presented in Figs. 1, S1, and S2. The normalized parameters were indicated by four principal components (PC), i.e., PC1 (33.8 %), PC2 (17.2 %), PC3 (12.2 %), and PC4 (11.5 %), with a total variance of 74.6 %. In the score plot, OCPs is positively aligned with PC1, whereas PCDDs and PCDFs are negatively correlated with PC1. PCBs and PBDEs positively respond to PC2 and OCPs; PCDDs and PCDFs negatively correlate with PC2. These results divide the organohalogen compounds in three clusters (OCPs, PCDD/Fs, and PCBs and PBDEs) (Fig. 1a).

In the loading plot, logKow, HOMO–LUMO gap, molecular weight, and TEF are negatively aligned with PC1. Total energy, q^- , and E_{LUMO} are positively aligned with PC1. LogBAF, final heat of formation, half-life, and total dipole are positively aligned with PC2. Finally, electronic energy and water solubility respond negatively to PC2 (Fig. 1b). Based on these results, the organohalogen compounds are divided into two categories: (a) PCBs and PBDEs and (b) OCPs and PCDD/Fs. PCBs and PBDEs are aligned with factors of bioconcentration (logBAF, logBCF, and half-life) and polarity (total dipole). PCDD/Fs are aligned with core–core repulsion, molecular weight, TEF, and OCPs aligned with water solubility (Fig. 1). The number of halogenated atom in PCBs, PBDEs, and PCDD/Fs aligns with factors of molecular weight (molecular weight, logKow, and logKoA). The maternal–fetal transfer rate is correlated positively with PC1, PC3, and PC4 and negatively with PC2 (Figs. 1b, S3, and S2), indicating that the maternal–fetal transfer rate of OCPs and lower chlorinated PCBs might be higher than that of PCDD/Fs and higher chlorinated PCBs.

Results of the MLR, PLS, and RF models

In accordance with Spearman-ranked correlation coefficient values (Table 2), one value is removed from each pair of eight redundant variables (logKow, logKoA, water solubility, half-life, total energy, electronic energy, core–core repulsion, and E_{LUMO}) presenting correlation coefficients greater than 0.7. The remaining 10 variables (molecular weight, TEF, logBCF, logBAF, final heat of formation, E_{HOMO} , q^- , q^+ , HOMO–LUMO gap, and total dipole) were selected for model development.

MLR and PLS models provide rather low predictive performance (Table 3), evaluated through the 10-fold cross-validation ($R^2_{CV} = 0.425 \pm 0.0964$ and $RMSE_{CV} = 0.0740 \pm 0.00962$ for MLR and $R^2_{CV} = 0.492 \pm 0.115$ and $RMSE_{CV} =$

Table 3 Prediction performance of the investigated maternal transfer rate for MLR, PLS, and RF models

	Internal validation ^a (24 compounds ^b)				External validation (7 compounds ^c)	
	RMSE	RMSE SD	R^2	R^2 SD	RMSE	R^2
MLR	0.0740	0.00962	0.425	0.0964	0.0897	0.129
PLS	0.0699	0.0109	0.492	0.115	0.112	0.123
RF	0.0648	0.00848	0.566	0.0885	0.0514	0.519

^a 10-fold cross-validation

^b 24 compounds: HCB, HCH, heptachlor epoxide, 1,2,3,7,8-PeCDD, 1,2,3,6,7,8-HxCDD, 1,2,3,4,6,7,8-HpCDD, OCDD, 2,3,4,7,8-PeCDF, 1,2,3,4,6,7,8-HpCDF, CB77, CB126, CB169, CB114, CB118, CB123, CB156, CB157, CB167, TetraCB, PentaCB, HexaCB, OctaCB, BDE47, and BDE153

^c 7 compounds: trans-nonachlor, 1,2,3,4,7,8-HxCDF, 1,2,3,6,7,8-HxCDF, CB105, CB189, HeptaCB, and BDE100

0.0699±0.0109 for PLS) and the external test set ($R^2_{pred}=0.129$ and $RMSE_{red}=0.0897$ for MLR and $R^2_{pred}=0.123$ and $RMSE_{pred}=0.112$ for PLS). In these models, the q^- , E_{HOMO} , and HOMO–LUMO gap are significant variables for the PLS; E_{HOMO} , TEF, molecular weight, and logBAF are selected for the MLR (Table 4).

The RF model provides better predictive performance, evaluated through the 10-fold cross-validation ($R^2_{CV}=0.566 \pm 0.0885$, $RMSE_{CV}=0.0648 \pm 0.00848$), the external test set ($R^2_{pred}=0.519$ and $RMSE_{pred}=0.0514$) (Table 3), and values of Tropsha’s validation factor fit into the standard ($R^2_{EXT}=0.508$, $k=1.033$, and $(R^2_{pred}-R^2_0)/R^2_{pred}=0.0062$). The value of the average of 100 random shuffles of R^2 ($R^2_{random}=0.532$) was lower than $R^2_{CV}=0.566$, indicating that the results from the proposed model were not due to chance correlation. The applicability was defined for the compounds that constituted the test compounds as described. Since half of the validation compounds fell inside the domain of applicability (Table 5), the reliability of this model from the APD was slightly low, meaning the RF model almost passed the tests for predictive ability, except for R^2_{pred} and domain of applicability. In RF model, total dipole, molecular weight, HOMO–LUMO gap, and E_{HOMO} are accepted as significant variables (Table 4).

Discussion

Prediction of the maternal–fetal transfer rates

Transfer rates of PCBs, OCPs, PBDEs, and dioxin-like compounds in this study were 0.124 to 0.235, 0.161 to 0.255, 0.125 to 0.238, and 0.109 to 0.326 on a wet wt basis, respectively. Previous study reported that transfer rates of PCBs, OCPs, PBDEs, and dioxin-like compounds were 0.1 to 0.4, 0.1 to 3, 0.05 to 5, and 0.1 to 0.4 on a wet wt basis, respectively (Aylward et al. 2014), indicating that cord/maternal blood concentrations in this study were the same level as previous report.

In this study, three prediction models are developed and compared, although their prediction accuracy is not expected to differ significantly (Kovdienko et al. 2010). Indeed, RF regression clearly offers greater prediction accuracy than the MLR and PLS models in this study. A previous study indicated that RF would be suitable for the analysis of small sample size, high-dimensional feature space, and complex data structures (Qi 2012). Sample size and the number of target compounds in the current study are smaller than in a previous research (Lancz et al. 2015). Indeed, RF proves a sufficient

Table 4 Important variables of MLR, PLS, and RF for prediction of maternal transfer rate

RF	PLS		MLR		<i>t</i> Value
	Variable importance		Variable importance		
Total dipole	100	LogBAF	100	Final heat of formation	−21.655
LogBCF	99.81	LogBCF	35.26	LogBAF	15.664
Molecular weight	71.141	$E_{HOMO}-E_{LUMO}$	28.657	Molecular weight	7.728
$E_{HOMO}-E_{LUMO}$	48.452	Total dipole	23.331	TEF	−7.028
E_{HOMO}	40.37	E_{HOMO}	17.026		
q^+	34.537	TEF	8.518		
Final heat of formation	13.598	Final heat of formation	3.854		
TEF	12.797	q^-	2.621		
q^-	7.289	q^+	2.058		
LogBAF	0	Molecular weight	0		

Table 5 Applicability domain for the test compounds

	Distance ^a (APD=0.109)
1.2.3.4.7.8.HxCDF	0.139
1.2.3.6.7.8.HxCDF	0.120
CB105	0.106
CB189	0.0819
HeptaCB	0.102
BDE100	0.183
Trans-nonachlor	0.143

^a Distance was calculated from the average predicted transfer rate for each compound of each maternal–fetal pairs

robust prediction model. However, because the kinds of data about OCP were limited, the transfer rate of OCPs was difficult to predict in our model. In the future, more data about OCPs are needed to develop a more accurate model. The total dipole parameters, signified in RF (Table 4), relate highly to the compounds' polarity. Previous reports supported that large polar molecules cross the placenta slowly, whereas lipophilic drugs pass more rapidly (Reynolds 1998) and the number of ionizable groups contributed negatively to the maternal–fetal transfer rate (Giaginis et al. 2009). It was also suggested that the topological polar surface area, q^+ , and the dipole moment influence the maternal–fetal transfer rate (Hewitt et al. 2007), indicating that it is difficult for high-polarity compounds to be transported to the fetus. Moreover, multidrug resistance proteins (MRPs) are known to mediate the transport of various glucuronides, xenobiotics, and their metabolites, including polar conjugates (Deeley et al. 2006), indicating that polarity of compounds might be crucial for the maternal–fetal transfer rate.

The logBCF and the molecular weight related to transfer rate in RF (Table 4). Compounds with higher molecular weight (approximately more than 500 Da) are expected to have transferred incompletely as they cannot penetrate the pores of the placental membrane (Audus 1999; Bourget et al. 1995; Hewitt et al. 2007; Koppe et al. 1992), indicating that molecular weight negatively correlates with maternal–fetal transfer rate. Previous studies also reported that logKow is significantly related to the maternal–fetal transfer rate and several physicochemical properties, such as molecular weight, water solubility, and the number and type of halogen group (Meylan and Howard 2000; Monteiro et al. 2008). In addition, fatty acids are suggested as a transporter for dioxin-like compounds (Koppe et al. 1992). In the present study, molecular weight is significantly correlated with logKow, logKoA, water solubility, total energy, core–core repulsion, E_{LUMO} , and HOMO–LUMO gap (Table 2). This suggests that molecular weight and/or lipophilicity are important parameters for the maternal–fetal transport of organohalogen compounds.

E_{HOMO} and HOMO–LUMO gap also related to transfer rate in the RF model (Table 4). It was reported that cytochrome P450 (CYPs) have been found in the human placenta (Pasanen 1999). CYPs are well-known xenobiotic enzymes and are responsible for the detoxification of drugs and xenobiotics. Lewis et al. have shown that binding to CYP3A4 is negatively dependent on the E_{HOMO} , indicating that compounds with a large HOMO energy tended to be difficult to metabolize by CYP3A (Lewis et al. 2002). In RF, TEF was selected as the predictive variable in this study and TEF negatively correlates with the maternal–fetal transfer rate; this is also confirmed by PCA in PC1 (Fig. 1b). The aryl hydrocarbon receptor (AhR) protein (Jiang et al. 2010) has been recorded in the human placenta, indicating that dioxin-like compounds may be binding AhR proteins (Manchester et al. 1987) and thus having difficulty transferring across the human placenta. Moreover, CYP1A1 is the major CYP isoform present in human placenta (Pasanen 1999). Placental CYP1A1 is induced by lifestyle factors such as smoking, environmental factors (including PCBs, dioxin-like compounds), and medications (e.g., azidothymidine and glucocorticoids) (Myllynen et al. 2005). Based on these results, it is hypothesized that organohalogen compounds might be a reduction by CYP metabolism and/or binding AhR proteins.

Further studies on organohalogen compound transporters are required to develop a prediction model for the maternal–fetal transfer rate. Several transporters are expressed in the human placenta such as ATP-binding cassette transporters, ATP-binding cassette sub-family G member 2 (ABCG2)/breast cancer resistance protein, ATP-binding cassette sub-family B member 1 (ABCB1)/P-glycoprotein, and ATP-binding cassette sub-family C member 2 (ABCC2)/multidrug resistance protein 2 (MRP2) (Myllynen et al. 2009; Vahakangas and Myllynen 2009); however, relations with organohalogen compounds and these transporters are still not completely understood. Thyroid hormone (TH) can cross the placenta to the fetus, and maternal thyroxine is crucial for the development of fetal brain; however, due to structural similarity of thyroxine, a possible mechanism involved in the disruption of TH homeostasis is the competitive binding of organohalogen compounds to the TH transport protein transthyretin (Marchesini et al. 2008), thyroid binding globulin, and albumin in blood (Ucan-Marín et al. 2010), indicating that organohalogen compounds may cross the placenta by TH transporters.

Conclusion

In this paper, we predict the maternal–fetal transfer rate of PCBs, OCPs, PBDEs, and dioxin-like compounds using multivariate analysis to detect relations between the physicochemical properties of these compounds and their maternal–fetal

transfer rate. RF regression clearly offers greater prediction accuracy than the MLR and PLS models to predict for maternal transfer rate and molecular weight, and/or lipophilicity might be important parameters for the maternal–fetal transport of organohalogen compounds. Further studies on organohalogen compound transporters are required to develop a prediction model for the maternal–fetal transfer rate including protein binding actively and metabolic rate of these compounds in placenta.

Acknowledgments These studies were supported by grants for Scientific Research (A): Grants-in-Aid for Scientific Research <KAKENHI (20241016)>, Scientific Research (B): Grants-in-Aid for Scientific Research <KAKENHI (24310021)>, Grant-in-Aid for Research Activity start-up (26881003) from the Japanese Ministry of Education Culture, Sports, Science and Technology, and the Environment Research and Technology Development Fund (5-1305) from the Ministry of the Environment of Japan.

References

Akaike H (1998) Information theory and an extension of the maximum likelihood principle. In: Parzen E, Tanabe K, Kitagawa G (eds) Selected papers of Hirotugu Akaike. Springer, New York

Ankley GT, Bennett RS, Erickson RJ, Hoff DJ, Hornung MW, Johnson RD, Mount DR, Nichols JW, Russom CL, Schmieder PK, Serrano JA, Tietge JE, Villeneuve DL (2010) Adverse outcome pathways: a conceptual framework to support ecotoxicology research and risk assessment. *Environ Toxicol Chem* 29:730–741

Audus KL (1999) Controlling drug delivery across the placenta. *Eur J Pharm Sci* 8:161–165

Aylward LL, Hays SM, Kirman CR, Marchitti SA, Kenneke JF, English C, Mattison DR, Becker RA (2014) Relationships of chemical concentrations in maternal and cord blood: a review of available data. *J Toxicol Environ Health Part B* 17:175–203

Bourget P, Roulot C, Fernandez H (1995) Models for placental-transfer studies of drugs. *Clin Pharmacokinet* 28:161–180

Breiman L (2001) Random forests. *Mach Learn* 45:5–32

Brouwer A, Ahlborg UG, Vandenberg M, Birnbaum LS, Boersma ER, Bosveld B, Denison MS, Gray LE, Hagmar L, Holene E, Huisman M, Jacobson SW, Jacobson JL, Koopmanesseboom C, Koppe JG, Kulig BM, Morse DC, Muckle G, Peterson RE, Sauer PJJ, Seegal RF, Smitsvanprooijje AE, Touwen BCL, Weisglaskuperus N, Winneke G (1995) Functional aspects of developmental toxicity of polyhalogenated aromatic hydrocarbons in experimental animals and human infants. *Eur J Pharmacol-Environ* 293:1–40

Deeley RG, Westlake C, Cole SPC (2006) Transmembrane transport of endo- and xenobiotics by mammalian ATP-binding cassette multi-drug resistance proteins. *Physiol Rev* 86:849–899

EPA (2012) U. Estimation Programs Interface Suite™ for Microsoft® Windows, v 4.11. United States Environmental Protection Agency, Washington, DC, USA

Fukata H, Omori M, Osada H, Todaka E, Mori C (2005) Necessity to measure PCBs and organochlorine pesticide concentrations in human umbilical cords for fetal exposure assessment. *Environ Health Perspect* 113:297–303

Giaginis C, Zira A, Theocharis S, Tsantili-Kakoulidou A (2009) Application of quantitative structure-activity relationships for modeling drug and chemical transport across the human placenta barrier: a multivariate data analysis approach. *J Appl Toxicol* 29: 724–733

Grandjean P, Landrigan PJ (2006) Developmental neurotoxicity of industrial chemicals. *Lancet* 368:2167–2178

Grandjean P, Landrigan PJ (2014) Neurobehavioural effects of developmental toxicity. *Lancet Neurol* 13:330–338

Hewitt M, Madden JC, Rowe PH, Cronin MTD (2007) Structure-based modelling in reproductive toxicology: (Q)SARs for the placental barrier. *SAR QSAR Environ Res* 18:57–76

Jiang YZ, Wang K, Fang R, Zheng J (2010) Expression of aryl hydrocarbon receptor in human placentas and fetal tissues. *J Histochem Cytochem* 58:679–685

Jotaki T, Fukata H, Mori C (2011) Confirmation of polychlorinated biphenyl (PCB) distribution in the blood and verification of simple quantitative method for PCBs based on specific congeners. *Chemosphere* 82:107–113

Kawashiro Y, Fukata H, Inoue MO, Kubonoya K, Jotaki T, Takigami H, Sakai SI, Mori C (2008) Perinatal exposure to brominated flame retardants and polychlorinated biphenyls in japan. *Endocr J* 55: 1071–1084

Koppe JG, Olie K, Vanwijnen J (1992) Placental transport of dioxins from mother to fetus. 2. PCBs, dioxins and furans and vitamin-K metabolism. *Dev Pharmacol Ther* 18:9–13

Kovdienko NA, Polishchuk PG, Muratov EN, Artemenko AG, Kuz'min VE, Gorb L, Hill F, Leszczynski J (2010) Application of random forest and multiple linear regression techniques to QSPR prediction of an aqueous solubility for military compounds. *Mol Inf* 29:394–406

Kuhn M (2008) Building predictive models in R using the caret package. *J Stat Softw* 28:1–26

Lancz K, Murínová E, Patayová H, Drobná B, Wimmerová S, Šovčíková E, Kováč J, Farkašová D, Hertz-Picciotto I, Jusko TA, Trnovec T (2015) Ratio of cord to maternal serum PCB concentrations in relation to their congener-specific physicochemical properties. *Int J Hyg Environ Health* 218:91–98

Lewis DFV, Modi S, Dickins M (2002) Structure-activity relationship for human cytochrome P450 substrates and inhibitors. *Drug Metab Rev* 34:69–82

Mably TA, Bjerke DL, Moore RW, Gendron-Fitzpatrick A, Peterson RE (1992) In utero and lactational exposure of male rats to 2,3,7,8-tetrachlorodibenzo-p-dioxin: 3 effects on spermatogenesis and reproductive capability. *Toxicol Appl Pharmacol* 114:118–126

Manchester DK, Gordon SK, Golas CL, Roberts EA, Okey AB (1987) Ah receptor in human placenta—stabilization by molybdate and characterization of binding of 2,3,7,8-tetrachlorodibenzo-para-dioxin, 3-methylcholanthrene, and benzo(a)pyrene. *Cancer Res* 47: 4861–4868

Marchesini GR, Meimaridou A, Haasnoot W, Meulenberg E, Albertus F, Mizuguchi M, Takeuchi M, Irth H, Murk AJ (2008) Biosensor discovery of thyroxine transport disrupting chemicals. *Toxicol Appl Pharmacol* 232:150–160

Meylan WM, Howard PH (2000) Estimating log P with atom/fragments and water solubility with log P. *Perspect Drug Discov* 19:67–84

Monteiro CJP, Pereira MM, Pinto SMA, Simoes AVC, Sa GFF, Arnaut LG, Formosinho SJ, Simoes S, Wyatt MF (2008) Synthesis of amphiphilic sulfonamide halogenated porphyrins: MALDI-TOFMS characterization and evaluation of 1-octanol/water partition coefficients. *Tetrahedron* 64:5132–5138

Mori C, Nakamura N, Todaka E, Fujisaki T, Matsuno Y, Nakaoka H, Hanazato M (2014) Correlation between human maternal-fetal placental transfer and molecular weight of PCB and dioxin congeners/isomers. *Chemosphere* 114:262–267

Myllynen P, Pasanen M, Pelkonen O (2005) Human placenta: a human organ for developmental toxicology research and biomonitoring. *Placenta* 26:361–371

Myllynen P, Immonen E, Kumm M, Vahakangas K (2009) Developmental expression of drug metabolizing enzymes and

- transporter proteins in human placenta and fetal tissues. *Expert Opin Drug Metab* 5:1483–1499
- Needham LL, Grandjean P, Heinzow B, Jorgensen PJ, Nielsen F, Patterson DG, Sjodin A, Turner WE, Weihe P (2011) Partition of environmental chemicals between maternal and fetal blood and tissues. *Environ Sci Technol* 45:1121–1126
- Pasanen M (1999) The expression and regulation of drug metabolism in human placenta. *Adv Drug Deliv Rev* 38:81–97
- Qi Y (2012) Random forest for bioinformatics. In: Zhang C, Ma Y (eds) *Ensemble machine learning*. Springer, US
- Reynolds F (1998) Drug transfer across the term placenta: a review. *Placenta* 19(Supplement 2):239–255
- Rucker C, Rucker G, Meringer M (2007) γ -Randomization and its variants in QSPR/QSAR. *J Chem Inf Model* 47:2345–2357
- Sakurai K, Todaka E, Saito Y, Mori C (2004) Pilot study to reduce dioxins in the human body. *Intern Med* 43:792–795
- Stewart JJP (2007) Optimization of parameters for semiempirical methods V: modification of NDDO approximations and application to 70 elements. *J Mol Model* 13:1173–1213
- Stewart JJP, MOPAC 2009 Version 9.03CS. *Stewart Computational Chemistry*. [HTTP://OpenMOPAC.net](http://OpenMOPAC.net); 2008
- Tropsha A (2010) Best practices for QSAR model development, validation, and exploitation. *Mol Inf* 29:476–488
- Ucan-Marin F, Arukwe A, Mortensen AS, Gabrielsen GW, Letcher RJ (2010) Recombinant albumin and transthyretin transport proteins from two gull species and human: chlorinated and brominated contaminant binding and thyroid hormones. *Environ Sci Technol* 44:497–504
- Vahakangas K, Myllynen P (2009) Drug transporters in the human blood-placental barrier. *Br J Pharmacol* 158:665–678
- Van den Berg M, Birnbaum LS, Denison M, De Vito M, Farland W, Feeley M, Fiedler H, Hakansson H, Hanberg A, Haws L, Rose M, Safe S, Schrenk D, Tohyama C, Tritescher A, Tuomisto J, Tysklind M, Walker N, Peterson RE (2006) The 2005 World Health Organization reevaluation of human and mammalian toxic equivalency factors for dioxins and dioxin-like compounds. *Toxicol Sci* 93:223–241
- Wold S, Sjostrom M, Eriksson L (2001) PLS-regression: a basic tool of chemometrics. *Chemom Intell Lab* 58:109–130
- Zhang SX, Golbraikh A, Oloff S, Kohn H, Tropsha A (2006) A novel automated lazy learning QSAR (ALL-QSAR) approach: method development, applications, and virtual screening of chemical databases using validated ALL-QSAR models. *J Chem Inf Model* 46:1984–1995